Evidence for a weakening of tropical surface wind extremes in response to atmospheric warming

Guillaume Gastineau and Brian J. Soden

Department of Meteorology and Physical Oceanography, Rosenstiel School for Marine and Atmospheric Science, Miami, Florida, USA

Guillaume Gastineau, Departement of Meteorology and Physical Oceanography, Rosenstiel School for Marine and Atmospheric Science, 4600 Rickenbacker Causeway, Miami, FL 33149, USA. (ggastineau@rsmas.miami.edu)

The changes of extreme winds and its links with precipitation are assessed over the past two decades using daily satellite observations and climate model simulations. Both observations and models indicate a decrease in the frequency of the strongest wind events and an increase in the frequency of light wind events in response to a warming of the tropical oceans. The heaviest precipitation events are found to be more frequent when the tropical oceans warm, but the surface winds associated with these extreme rainfall events weaken. These results add further evidence to suggest that the atmospheric circulation becomes less energetic as the climate warms. It further suggests that the enhancement of the extreme precipitation events is mainly a result of increasing atmospheric water vapor and occurs despite a weakening of the large-scale circulation, which acts to diminish the mass convergence toward the precipitating zones.

1. Introduction

Climate models predict that the atmospheric circulation will weaken as the climate warms in response to rising greenhouse gases [*Held and Soden* 2006; *Vecchi and Soden*, 2007; *Chou and Chen*, 2010]. This weakening results from a slower rate of increase in global-mean precipitation compared to global-mean water vapor; the latter increasing at a rate of roughly 7% per degree of surface warming — consistent with expectations from the Clausius-Clapeyron equation in which changes in relative humidity are small compared to the increase in equilibrium vapor pressure. Precipitation is constrained by radiative budget considerations to increase at a slower rate of 3%/K [*Stephens and Ellis*, 2008].

The imbalance between the scaling of global precipitation and global water vapor, and the resulting weakening of the atmospheric circulation is a robust projection of all climate models [*Held and Soden*, 2006]. This weakening is primarily manifest as a reduction in the zonally-asymmetric (i.e., Walker cell) component of the tropical circulation, associated to a shoaling and relaxation of the thermocline, an eastward shift of atmospheric convection, and a drift of the mean-climate towards a more "El Niño" like state [*Vecchi and Soden*, 2007]. However, the corresponding SST anomalies in the Equatorial Pacific region are much smaller than those associated to global warming.

At the surface, the model-projected weakening of the mean circulation is manifest as a reduction in both the mean wind speed and the frequency of the strongest wind storms. *Gastineau and Soden* [2009] found that the frequency of extreme wind events decreased over the tropics as the climate warms. Heavy precipitation events became more common in a warmer climate, but were found to be associated with weaker upward vertical velocities, as found by *O'Gorman and Schneider* [2009]; *Sugiyama et al.* [2010].

Observational evidence to confirm or refute these model projections is limited and controversial. Using data collected from ship measurements, *Vecchi et al.* [2006] found a pattern of sea level pressure change over the past century that is consistent with a weakening of the Walker circulation. Observations of ocean wave height [*Gulev and Grigorieva*, 2004] show a pattern of increasing wave heights over the extratropics and decreasing wave heights over the tropics, consistent with model projected changes in surface winds [*Gastineau and Soden*, 2009]. More recently, changes in the isotopic composition of corals in the western Pacific suggest a shoaling of the thermocline over the past century consistent with a weakening of the Walker circulation [*Williams and Grottoli*, 2009].

On the other hand, *Wentz et al.* [2007] showed from SSM/I satellite estimates that precipitation has increased at the same rate as the total column water vapor over the past two decades, implying that there should be no change in the mean atmospheric circulation. Similar discrepancies between the rate of observed and model-predicted precipitation changes have been found by others [*Allan and Soden*, 2008; *Zhang et al.*, 2007; *Liepert and Previdi*, 2009].

In this paper, we use a 20 year record of surface wind speed measurements from the Special Sensor Microwave/Imager (SSM/I) and outputs from the climate models. We show that both observations and models indicate a reduction in the strongest wind events in response to a warming of the tropical oceans. The data and methods are described in section 2, followed by an analysis of the mean and extreme wind responses to tropical warming in sections 3 and 4. A summary and discussion of the implications of these results is presented in section 5.

2. Data and Methods

Twice-daily SSM/I wind and precipitation are downloaded with a horizontal resolution of 0.25°x0.25° [*Wentz et al.*, 2007]. These products provide estimates of wind and precipitation over ocean, from satellite microwave measurements. For comparison with coarser climate model grids, the observational data set were degraded to 2.5°x2.5° resolution, while ascending and descending overpasses were averaged into daily data. As the orbital drift of the satellites may introduce a spurious trend due a drift in the diurnal sampling, we use only the satellites f08, f11 and f13 that have the most stable orbit (see auxiliary materials). For a better accuracy, we mask out the coastal grid points, and the winds if precipitation occurs over the surrounding pixels.

The daily surface winds and precipitation of atmospheric-only and coupled model simulations are obtained from the CMIP3 (Coupled Model Intercomparison Project Phase 3) archive. A set of AMIP (Atmospheric Model Intercomparison Project) experiments is included, in which 11 atmospheric models are forced with observed SSTs. We also analyze a set of 18 ocean-atmosphere model experiments, using the 20th century scenario in which the observed anthropogenic and natural forcings are used. The surface wind intensity in model is computed as the norm of the surface wind vector, and is also regridded into 2.5°x2.5° resolution data. Unless stated otherwise, all data over land are set to undefined values, in order to be consistent with the ocean-only satellite observations.

3. The changes of wind intensity over the recent period

Figure 1 (left panels) illustrates the mean wind over the tropical region for SSM/I observations and the AMIP and coupled multi-model means. The largest wind values are obtained in the trade wind core, near the eastern part of the oceanic basins, where the SST gradients are the strongest. A minimum is seen at the thermal equator and over the warm pool region, where the SST gradients are weak. The surface wind distribution in models and observations are quite similar, even if the mean wind is weaker in models.

The monthly wind speed at each grid point was regressed onto the mean tropical SST, between 30°N and 30°S, using the Optimum-Interpolation (OI) SST dataset [*Reynolds et al.*, 2002], AMIP SSTs or the individual SST outputs of each coupled model.

Figure 1 (right panels) shows the wind changes obtained in response to a tropical SST warming of 1K. For SSM/I winds, a statistical test is built with a Monte Carlo approach to study the confidence level of the regression. We calculate the regression onto the tropical-mean SSTs of 1000 random permutations of the wind time series. The permutations are performed by block of 3 months, to reduce the influence of serial autocorrelation. The significance of the test is determined with the percentage of randomized regressions that exceeds the regression being tested. In the SSM/I observations, a significant decrease of the wind is observed over the Central Equatorial Pacific, while the Pacific Ocean trade winds are more intense over 15° in both hemispheres. These changes are mainly due to the warming induced by El Niño Southern Oscillation (ENSO), with a Gill-like response to enhanced convection in the Central Equatorial Pacific. This response induces a pair of off-equatorial cyclones, which amplifies the easterlies around 15° and reduces the equatorial easterlies (see auxiliary materials). The winds are also amplified over the eastern Pacific Ocean as the meridional temperature gradient increases in response to ENSO. The SSM/I data also shows a significant decrease of the trade winds over the Indian and Atlantic Ocean.

The AMIP model wind changes have a structure similar to observations, however the changes over Eastern Pacific, Indian and Atlantic Ocean are less marked, while the intensification of the winds over the Northern Pacific is larger than the observations. The coupled models also reproduce a structure similar to the one observed, but there are important differences over the eastern Pacific Ocean, as decadal variability is smoothed in the coupled multi-model mean. Model errors are also amplified by the ocean-atmosphere coupling.

4. Change in the extreme wind events and links with precipitation

The occurrence of precipitation and wind events is computed for satellite and model winds. First, the percentiles of daily wind and precipitation are calculated for the period 1987-1990, over the tropical region (30°N-30°S). For each month (m), of each year (y), we obtain a fraction f of grid points falling within the 0-10%, ..., 90-95%, 95-99% and 99-100% percentile bins (b). A percentage anomalous frequency is calculated as a function of time and bin:

$$F(y,m,b) = 100(f(y,m,b) - \overline{f(m,b)}^{y} / \overline{f(b)}^{y,m}) \tag{1}$$

where anomalies from the seasonal cycle are normalized by the mean frequency of each percentile. The overbars indicate a yearly (y) or temporal average (y,m).

The anomalous frequency of the winds for each percentile bin is shown in Fig. 2 (upper panel) for the SSM/I observations, the results being smoothed with a 6-month running mean to highlight the interannual variability. The strongest winds become less frequent and lightest winds become more frequent as the oceans warm during El Niño conditions (e.g., during December 1987, the early 1990s and 1998). The opposite is generally true for La Niña events (e.g., 1989 and 1999). However, there are also substantial shifts in the distribution of the surface wind speed that are uncorrelated with ENSO activity, indicating that other sources of variability also contribute to the changes in wind speed. Due to ensemble averaging, the amplitude of the variability is lower in AMIP models (Fig. 2, lower panel). The distribution of winds in these models exhibits some similar behavior to observations for 1995-2000, however models fail to represent the strong 1989 La Niña signal.

To more clearly highlight the response to tropical ocean warming, the anomalous frequencies of wind and precipitation are regressed against the tropical-mean SST in Fig. 3, the significance level being estimated as illustrated previously. The grey shades indicate where the significance level is higer than 5%, and trends which lie outside these lines are assessed to be significant at the 95% level. Consistent with *Allan and Soden* [2008], we find that the distribution of precipitation shifts towards more extreme precipitation in response to warmer tropical SSTs. Specifically, the heaviest 1% precipitation (99-100% bin) become 20% more frequent for each 1K increase in tropical SST. Both the AMIP and CMIP-3 models exhibit a qualitatively similar behavior, even if the intermodel spread is quite large.

The anomalous wind frequency for SSM/I also indicates that warmer oceans are associated with less frequent strong wind events (95-100% bins) and more frequent weak events (20-30% bins). The largest sensitivity is observed for the strongest wind events (99-100% bin) which decrease by more than 20% for each 1K increase in tropical-mean SST. The AMIP and CMIP3 models also simulate more frequent weak winds (0-20% bins) and less frequent strong winds (99-100% bins), even if these changes are not significant. However, the strong-moderate winds (70-95% bins) are more frequent, while the weak-moderate winds (20-70% bins) are less frequent.

To investigate the links between precipitation and surface wind more directly, the daily wind speeds are averaged for each month separately within each of the precipitation percentile bin. In average, the heavy rainfalls are associated with stronger surface wind in the observations (Fig. 4, left panel). For the models, the strongest winds occur for the weak-moderate rainfall (30-50% bins) and the heaviest rainfall (99-100% bin). The monthly standard deviation of the observed winds (dashed lines) indicates that the links between surface wind and rainfall are quite stable over the whole period.

The largest sensitivity of the wind speed to surface warming is found for the heaviest precipitation events, as indicated by the tropical-mean SST regressions (Fig. 4, right panel). In both AMIP models and observations, the strongest precipitation events (80-100% bins) exhibit, on average, a significant decrease in the surface wind speed. The wind change associated with heavy precipitation is less important for the coupled models, however a reduction of the wind corresponding to heavy precipitation events is found, and this reduction exceeds the intermodel standard deviation. This result suggests that the intensification of the precipitation extremes is primarily driven by the thermodynamic factors (e.g., increased water vapor) rather than by dynamic changes (e.g., increased vertical mass flux), as found by [*Allan and Soden*, 2008; *O'Gorman and Schneider*, 2009].

The same analysis was repeated for coupled models using both ocean and land grid points (dashed blue line in Figs. 3 and 4). The anomalous frequency of rainfall and wind extremes are only slightly smaller over both ocean and land, suggesting that the same processes also occur over land in models, but with a weaker amplitude.

5. Discussion and conclusions

The observations and models indicate a decrease in the frequency of the strongest wind events and an increase in the frequency of light wind events in response to a warming of the tropical oceans. In surface wind observations, we found that the heaviest 1% precipitation events are 20% more frequent when the tropical oceans warm by 1K, but the surface winds associated with these extreme rainfalls weaken by almost 1 m s^{-1}. These results add further evidence to suggest that the atmospheric circulation becomes less energetic as the climate warms [*Hernández-Deckers and von Storch*, 2010]. It is consistent with model projections which suggest that a warmer climate is associated with a weakening of the tropical atmospheric circulation and a reduction in the frequency of the strongest wind events [*Gastineau and Soden*, 2009] that have important consequences on rainfall, along with the increasing water vapor concentration [*Seager et al.*, 2010].

A word of caution is required, as the results obtained using the mean tropical SST anomalies may be specifically linked to the interannual variability (ENSO), as the analogy between ENSO and global warming is limited. For instance, ENSO and global warming show different processes regarding the zonal atmospheric circulation anomalies in the subtropics [*Lu et al.*, 2008] or the impacts of the circulation anomalies onto precipitation [*Chou and Tu*, 2008]. However, the thermodynamic arguments presented for a weakening of the atmospheric circulation due to surface warming [e.g., *Held and Soden*, 2006] apply to both internal and externally-forced changes in climate. Indeed, the amplification of precipitation extremes and the associated weakening of the strongest winds is found for both El Niño events and the linear trends (see auxiliary materials).

The decrease of wind in response to a surface warming is well significant in wind observations, but it is smaller and less significant in models. This disagreement need to be further investigated. It may be linked the resolution, or the radiative forcing of clouds and aerosols [*Liepert and Previdi*, 2009; *Stephens and Ellis*, 2008]. Furthermore, the changes linked to the tropical storms and cyclones are not accounted for in the models where the resolution is not high enough, and it is expected that these events may be less frequent in global warming conditions [*Emanuel et al.*, 2008].

Acknowledgments. This work was supported by the NOAA Climate Program Office. SSM/I data are produced by Remote Sensing Systems and sponsored by the NASA Earth Science MEaSUREs DISCOVER Project. Data are available at www.remss.com. We acknowledge the modeling groups, the PCMDI and the WCRP working group on coupled modeling for their roles in making available the CMIP3 dataset. Support of this dataset is provided by the Office of Science, U.S. Department of Energy.

References

Allan, R. P., and B. J. Soden, Atmospheric warming and the amplification of precipitation extremes, *Science*, *321*(5895), 1481–1484, doi:10.1126/science.1160787, 2008.

Chou, C., and C.-A. Chen, Depth of convection and the weakening of tropical circulation in global warming, *J. Climate*, *23*(11), 3019–3030, 2010.

Chou, C., and J.-Y. Tu, Hemispherical Asymmetry of tropical precipitation in ECHAM5/MPI-OM during El Niño and under global warming, *J. Climate*, *21*(6), 1309–1332, 2008.

Emanuel, K., R. Sundararajan, and J. Williams, Hurricanes and global warming: results from downscaling IPCC AR4 simulations, *Bull. Am. Meteorol. Soc.*, *89*(3), 347–367, 2008.

Gastineau, G., and B. Soden, Model projected changes of extreme wind events in response to global warming, *Geophys. Res. Lett.*, *36*, L10810, doi:10.1029/2009GL037500, 2009.

Gulev, S. K., and V. Grigorieva, Last century changes in ocean wind wave height from global visual wave data, *Geophys. Res. Lett.*, *31*, L24302,doi:10.1029/2004GL021040, 2004.

Held, I. M., and B. J. Soden, Robust responses of the hydrological cycle to global warming, *J. Climate*, *19*, 5686–5699, 2006.

Hernández-Deckers, D., and J.-S. von Storch, Energetics responses to increases in greenhouse gas concentration, *J. Climate*, *23*(14), 3874–3887, 2010.

Liepert, B., and M. Previdi, Do models and observations disagree on the rainfall response to global warming?, *J. Climate*, *22*(11), 3156–3166, 2009.

Lu, J., G. Chen, and D. M. W. Frierson, Response of the zonal mean atmospheric circulation to El Niño versus global warming, *J. Climate*, *21*, 5835–5851, 2008.

O'Gorman, P., and T. Schneider, The physical basis for increases in precipitation extremes in simulations of 21st-century climate change, *Proc. Nat. Acad. Sci. USA*, *106*(35), 14,773–14,777, 2009a.

Reynolds, R., N. Rayner, T. Smith, D. Stokes, and W. Wang, An improved in situ and satellite SST analysis for climate, *J. Climate*, *15*, 1609–1625, 2002.

Seager, R., N. Naik, and G. A. Vecchi, Thermodynamic and dynamic mechanisms for large-scale changes in the hydrological cycle in response to global warming, *J. Climate*, *23*(17), 4651–4668, 2010.

Stephens, G., and T. Ellis, Controls of global-mean precipitation increases in global warming GCM experiments, *J. Climate*, *21*(23), 6141–6155, 2008.

Sugiyama, M., H. Shiogama, and S. Emori, Precipitation extreme changes exceeding moisture content increases in MIROC and IPCC climate models, *Proc. Nat. Acad. Sci. USA*, *107*(2), 571–575, 2010.

Vecchi, G., and B. Soden, Global warming and the weakening of the tropical circulation, *J. Climate*, *20*, 4316–4340, 2007.

Vecchi, G. A., B. J. Soden, A. T. Wittenberg, I. M. Held, A. Leetmaa, and M. J. Harrison, Weakening of the tropical atmospheric circulation due to anthropogenic forcing, *Nature*, *441*, 73–76, 2006.

Wentz, F. J., L. Ricciardulli, K. Hilburn, and C. Mears, How much more rain will global warming bring?, *Science*, *317*(5835), 233–235, 2007.

Williams, B., and A. Grottoli, Recent shoaling of the nutricline and thermocline in the western tropical Pacific, *Geophys. Res. Lett.*, *37*, L22601, doi:10.1029/2010GL044867, 2009.

Zhang, X., F. W. Zwiers, G. C. Hegerl, F. H. Lambert, N. P. Gillett, S. Solomon, P. A. Stott, and T. Nozawa, Detection of human influence on twentieth-century precipitation trends, *Nature*, *448*, 461–465, 2007.

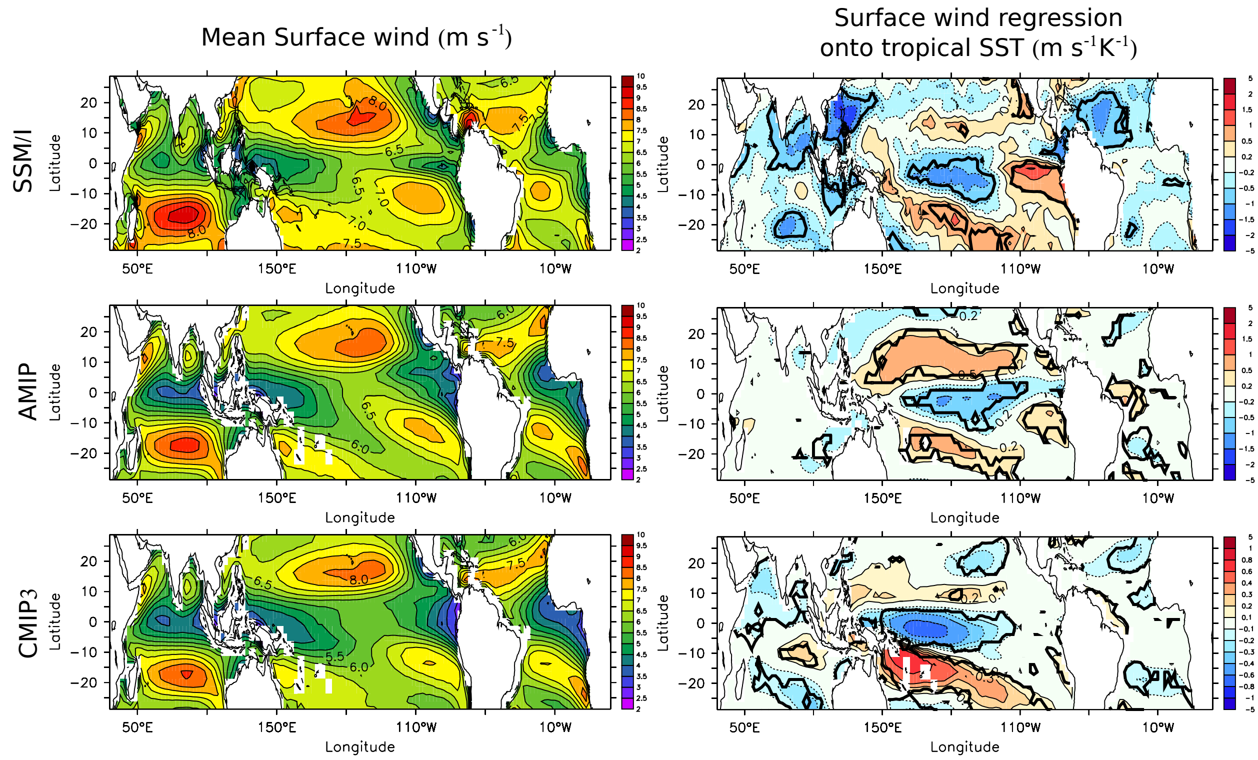

Figure 1. (Left panel) Mean surface wind in m s^{-1} and (right panel) regression of surface wind onto the mean tropical temperature (30°N-30°S), for (upper panel) SSM/I observations over the 1987-2008 period, and (middle panel) AMIP and (lower panel) coupled multi-model mean, over 1979-2000. In upper-right panel, thick contours indicate where the regression is 5% significant, as given by random permutations of the wind time series. In center-right and lower-right panels, thick contours illustrate the regions where more than 8 (13) AMIP (coupled) models show a change with the same sign as the multi-model mean.

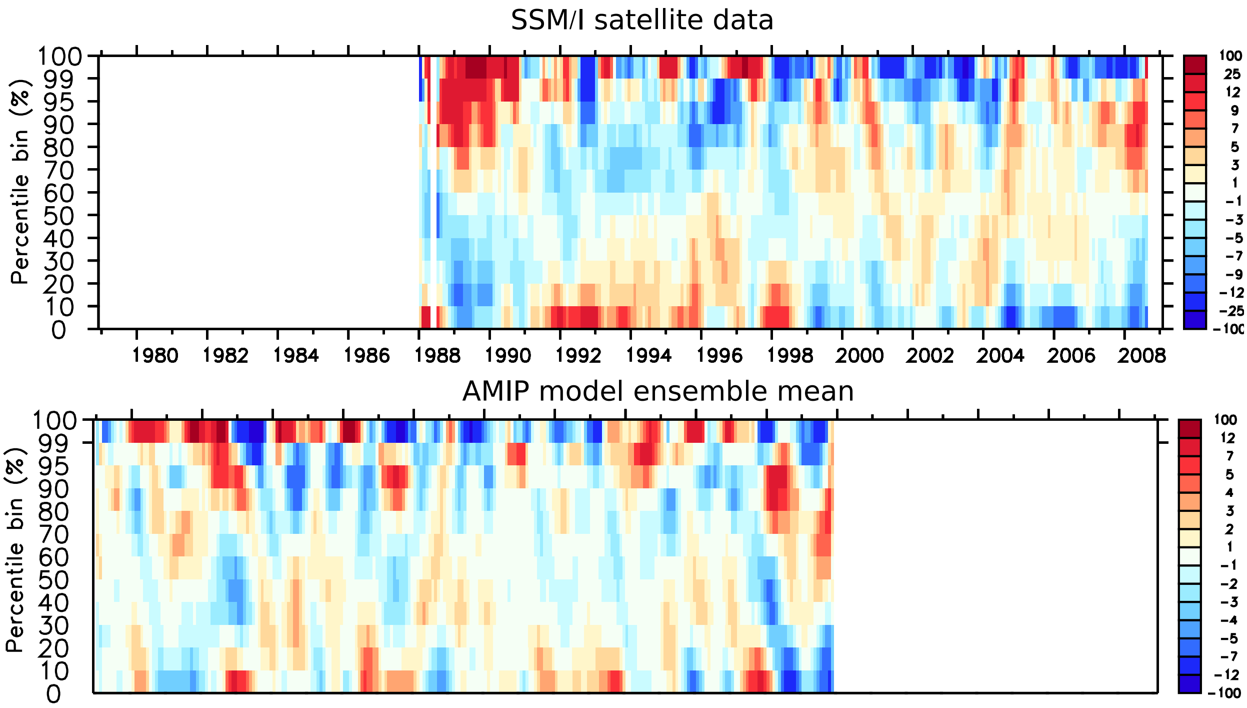

Figure 2. (Upper panel) Anomalous frequency of the wind, in %, in the SSM/I observations, smoothed by a 6-month running mean. (Lower panel) Same as top panel, but for the AMIP multi-model mean. Note that the color scale is different for upper and lower panels.

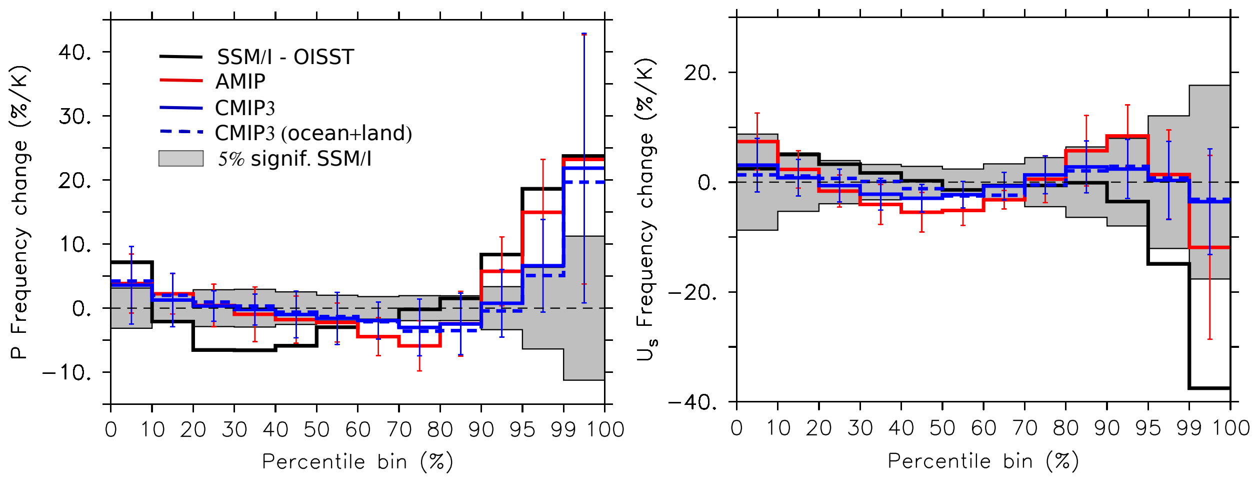

Figure 3. (Left) Regression of the precipitation and (right) wind anomalous frequency onto the mean tropical SST, in %/K, for SSM/I, AMIP and coupled multi-model mean. Grey shades indicate where the significance level of the regression from SSM/I is higher than 5%, as given by random permutations. The error bars show the standard deviations among AMIP and coupled models.

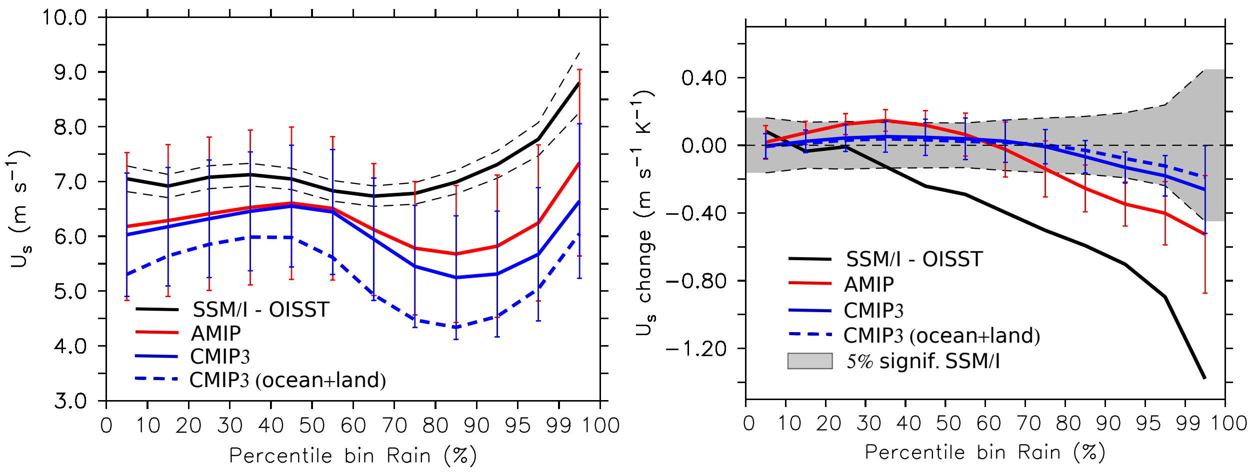

Figure 4. (Left) Mean wind in m s^{-1} and (right) regression of the wind onto the mean tropical SST in m s^{-1} K^{-1}, averaged over rain percentile bins, for SSM/I, AMIP and coupled multi-model mean. Thin dashed lines in left panel indicate the monthly standard deviation for the SSM/I wind data. Grey shades indicate where the significance level of the regression from SSM/I is higher than 5%, as given by random permutations. The error bars show the standard deviations among AMIP and coupled models.